Regulation of signal transduction pathways by hypoxia in breast cancer subtypes

Liu, Q.

Chapter 3

Differential response of luminal and basal breast cancer cells to acute and chronic hypoxia

Qiuyu Liu, Nasi Liu, Vera van der Noord, Wanda van der Stel, Bob van de Water, Erik H.J. Danen[#], Sylvia E. Le Dévédec[#]

[#] Co-corresponding authors
Submitted

Chapter 3

Abstract
Hypoxia is linked to disease progression and poor prognosis in several cancers, including breast cancer. Cancer cells can encounter acute, chronic and/or intermittent periods of oxygen deprivation and it is poorly understood how the different breast cancer subtypes respond to such hypoxia regimes. Here, we assessed the response of representative cell lines for the luminal and basal A subtype to acute and chronic hypoxia. High throughput targeted transcriptomics analysis showed that HIF related pathways are significantly activated in both subtypes. Indeed, HIF1α nuclear accumulation and induction of the HIF1α target, CA9 was similar. Based on the number of differentially expressed genes, i) 5 days exposure to hypoxia induced a more profound transcriptional reprogramming than 24 hours exposure and ii) basal A cells were less affected by acute and chronic hypoxia as compared to luminal cells. Hypoxia-regulated gene networks were identified of which hub genes were associated with worse survival in patients. Notably, while chronic hypoxia altered regulation of the cell cycle in both cell lines, it induced two distinct adaptation programs in these subtypes. Chronic hypoxia affected genes controlling central carbon metabolism in the luminal cells whereas in basal A cells genes controlling the cytoskeleton were affected. In agreement, lactate secretion was increased more prominently in luminal cell lines and three luminal cell lines upregulated GAPDH protein in response to chronic hypoxia while none of the basal A cell lines did. In contrast, basal A cells displayed enhanced cell migration associated with more F-actin stress fibers whereas luminal cells did not. Altogether, this data shows distinct responses to acute and chronic hypoxia that differ considerably between luminal and basal A cells and may play a role in the progression of these different breast cancer subtypes.

Keywords: Breast cancer, acute hypoxia, chronic hypoxia, luminal, basal

Introduction

Breast cancer remains the second leading cause of mortality in women [1]. Breast cancer can be divided into different subtypes including luminal A and B, basal-like (basal A and B) and HER-2 positive. Altered metabolism and increased invasiveness are two hallmarks of cancer, which both contribute to tumor progression and crosstalk [2,3]. Hypoxia, a key feature in growing solid tumors regulates both hallmarks and is therefore associated with an aggressive phenotype of breast cancer.

Hypoxia controls the expression of hundreds of genes involved in critical processes such as metabolism [4], cell motility [5] and epithelial-to-mesenchymal transition (EMT) [6] in breast cancer. This transcriptional regulation is tightly orchestrated by hypoxia-inducible factors (HIFs), transcription factors whose activity is sensitive to hypoxic stress [7]. HIFs comprising an alpha subunit (oxygen sensitive) and beta subunit (constitutively expressed) bind to hypoxia response elements (HREs) in the genome, regulating the cellular response to hypoxia [8]. The tissue microenvironment of breast tumors is highly heterogeneous and, depending on the local extent of newly formed blood vessels, it can contain regions of acute, intermittent and chronic hypoxia [9]. This is relevant as cancer cells show different cellular responses depending on the duration and frequency of hypoxia exposure [8,10]. Acute hypoxia is associated with reversible changes, chronic hypoxia is associated with long-term cellular changes potentially developing into mutagenesis and genetic instability [8].

The function of HIFs depends on both the level of oxygen deprivation and the duration of the hypoxic insult, and, consequently, their activities vary between acute and chronic hypoxia [7,9,11]. In addition, the type of hypoxia also influences the response of the tumor microenvironment. For example, acute hypoxia leads to endothelial cell death and microvascular permeability associated with increased lung metastasis of breast cancer cells whereas chronic hypoxia ultimately stimulates endothelial cell proliferation and vascular integrity which delays metastasis [12]. These findings indicate that the duration of hypoxic insults may represent an important factor in the progression of breast cancer that has not been fully explored. In addition, it is poorly understood if different breast cancer subtypes may be differently influenced by hypoxia.

To address these issues, in this study we focused on the luminal and basal A subtypes that share a predominantly epithelial morphology, in contrast to triple negative breast cancer (TNBC) cells that are typically more mesenchymal [13,14]. Hypoxia-induced EMT is associated with increased tumor cell motility [15] and high glycolytic activity [16], and TNBC cells display such EMT phenotypes. Using transcriptomics analysis, we identify shared and distinct responses to acute versus chronic hypoxia for luminal versus basal cells. Most notably, an initial shared HIF1α- response to acute hypoxia is followed by distinct metabolic versus migratory responses to chronic hypoxia in luminal and basal cells, respectively. Our findings shed new light on the response of different breast cancer subtypes to different regimes of hypoxia that may point to actionable mechanisms driving disease progression.

Material and methods

Cell culture

Human breast cancer cell lines (luminal: MCF-7, T47D, BT474; basal A: SUM149PT, HCC1806 and HCC1143) were obtained from American Type Culture Collection (ATCC). Cells were cultured in RPMI-1640 medium (#52400; Gibco, Waltham, MA, USA) with 10% FBS, 25 U/mL penicillin and 25 µg/mL streptomycin (#15140122; Gibco) in an incubator at 37°C with 5% CO_2 and 21% O_2 (normoxia) or 1% O_2 (hypoxia).

Human whole transcriptome analysis (TempO-Seq)

Targeted whole transcriptome analysis was performed using TempO-Seq [17] (BioSpyder Technologies Inc., Carlsbad, CA, USA). 3000-7000 cells/well of MCF-7 and HCC1143 were seeded in 96-well plates. Cells were lysed in 1× BioSpyder lysis buffer after 24 hrs or 5 days incubation under normoxia or hypoxia. Samples from three biological replicates were stored at -80°C and shipped to BioSpyder for TempO-Seq. An in-house R script was used for count normalization and determining differential gene expression. The library size (total number of reads per sample) was set as 100.000 reads and samples below this size were removed. DESeq2 package was used for count data normalization, adjusted p-value (padj) and $\log_2$Foldchange data. Differentially expressed genes (DEGs) were selected by $|\log_2\text{Foldchange}| > 1$ and padj <0.05. Given the high number of DEGs in the HCC1143 5-days dataset, in this case $|\log_2\text{Foldchange}| > 2$ and padj <0.01 was used for subsequent further analysis using bioinformatics tools. Heatmaps and Venn diagrams were made using OmicStudio tools at https://www.omicstudio.cn/tool.

Immunofluorescence

Cells were fixed with 4% paraformaldehyde and 0.3% Triton X-100, washed with PBS, blocked with 0.5% Bovine Serum Albumin (BSA) for 30 mins at room temperature, and stained with HIF1α antibody (#610959; BD Biosciences, Franklin Lakes, NJ, USA) and Rhodamin Phalloidin (R415; Thermo Fisher Scientific, Waltham, MA, USA) overnight at 4°C and 2 hrs at RT, respectively. Cells were rinsed with 0.5% BSA every 10 mins for 3 times and stained with secondary antibody and Hoechst 33258 (#610959; Thermo Fisher) for 1 hour at room temperature (RT) in the dark. After washing with PBS plates were stored at 4°C. Images were taken with Nikon Eclipse Ti microscope with 20× objective. Scale bars shown in images is 50 µm.

Western blotting

MCF-7 and HCC1143 cells were seeded at densities leading to subconfluency at the time of analysis and cultured under normoxia and hypoxia for 24 hrs and 5 days. Then, cells were lysed with RIPA buffer containing 1% protease/phosphatase inhibitor cocktail (P8340; Sigma-Aldrich, Burlington, MA, USA). The protein concentration was measured by BCA assay. Protein lysates were separated by SDS-PAGE and transferred to PVDF membranes. Membranes were blocked with 5% BSA and incubated with Carbonic Anhydrase IX antibody (5649S; Cell Signaling Technology, Danvers, MA, USA), PLOD2 antibody (MAB4445; R&D Systems, Minneapolis, MN, USA), glyceraldehyde 3-phosphate dehydrogenase (GAPDH) antibody (sc-32233; Santa Cruz, Dallas, TX, USA), or β-actin antibody (sc-47778; Santa Cruz) overnight at 4°C. Membranes were washed and incubated with HRP- or Cy5-conjugated secondary antibodies and signals were detected with an Amersham Imager (GE Healthcare Life Science, Chicago, IL, USA). Quantification of bands was done by Image J.

RT-qPCR

Total RNA was isolated by RNeasy Plus Mini Kit (#74136; Qiagen, Hilden, Germany) and cDNA was synthesized by the RevertAid H Minus First Strand cDNA Synthesis Kit (Thermo Fisher Scientific, Waltham, MA, USA). qPCR was performed using SYBR Green PCR master mix (Thermo Fisher Scientific) on a Real-Time PCR instrument (Applied Biosystems, Waltham, MA, USA). The following qPCR primer sets were used: β-actin forward (fw), 5'- ATTGCCGACAGGATGCAGAA -3'; β-actin reverse (rev), 5'- GCTGATCCACATCTGCTGGAA-3'; CA9 forward (fw), 5'- CATCCTAGCCCTGGTTTTTGG-3'; CA9 reverse (rev), 5'- GCTCACACCCCTTTGGTT-3'; PLOD2 forward (fw), 5'- GCGTTCTCTTCGTCCTCATCA-3'; PLOD2 reverse (rev), 5'- TGAAGCTCCAGCCTTTTCGTG-3'. Relative gene expression was calculated by $2^{-\Delta\Delta CT}$ method.

Lactate assay

Cells were cultured under normoxia and hypoxia for 24 hrs and 5 days, and supernatant medium was collected. 10 µL of supernatant medium was added into 96-well plates in each well, and 90 µL of reagent mix (80% TRAM buffer (108 mM Triethanolamine HCl (T9534; Sigma, Burlington, MA, USA), 10.7 mM EDTA-Na2 (E4884; Merck, Burlington, MA, USA), 42 mM $MgCl_2$ (M8266; Merck) in ddH_20, pH 7.5.), 20% colour reagent (1.63 mM PMS (P9625; Merck), 3.95 mM INT (I8377; Merck), 35% ethanol, and 2% Triton X-100 (T8787; Sigma-Aldrich)), 3.3 mM β-NAD (N7004; Merck) and 0.33 µL/mL LDH (L2500; Merck)) was added. Plates were incubated for 7 min at RT avoiding light. Optical density was measured in a plate reader at 490 nm and lactate was quantified against a lactate standard curve (#71718; Fluka Chemika, Buchs, Switzerland) using the abc-formula ($ax^2 + bx + c = 0$).

Sulforhodamine B (SRB) assay

Plates used for lactate assay, were subsequently fixed with 50% TCA for 1 hour at 4°C, washed with demi-water and air dried at RT. 0.4% SRB was added to plates and incubated for 2 hrs avoiding light at RT. Plates were washed with 1% acetic acid at least 5 times every 1 hour to get rid of unbound SRB and air dried. 10 mM Tris was added into wells to extract protein and plates were incubated for 2 hrs avoiding light at RT with gently shaking. The absorbance was measure by a plate reader (Tecan Infinite M1000, Männedorf, Switzerland).

Cell migration quantification assay

3000-7000 cells/well of MCF-7 and HCC1143 were seeded in 20 µg/mL collagen-coated 96-well plates. After 24 hrs or 5 days under normoxia or hypoxia medium was supplemented with 1:10000 Hoechst (#33242; Thermo Fisher) and images were taken every 10 mins using a Nikon Eclipse Ti microscope and O_2 controlled environment at 21% O_2 or at 1% O_2 using a 20x objective. Image analysis was performed using CellProfiler [18] and Rscript [19].

siRNA-mediated gene knockdown

50nM SMARTpool siRNA (Dharmacon, Lafayette, CO, USA) was transfected into cells using INTERFERin (Polyplus, Illkirch-Strasbourg, France). A KinasePool mixture containing >100 siRNAs targeting kinases with a total siRNA concentration of 50 nM (i.e., <0.5nM of each individual siRNA) was used as control. 3000-7000 cells/well of

MCF-7 and HCC1143 were seeded in 96-well plates and 8×10^4 - 10×10^4 cells/ well were seeded in 12-well plates. Medium was refreshed after 18hrs.

Cell cycle analysis using FUCCI reporter cell lines

MCF-7 and HCC1143 cells were transfected with pLL3.7m-Clover-Geminin (1-110)-IRES-mKO2-Cdt (30-120) (#83841; Addgene, Watertown, MA, USA). Transfected cells were enriched by fluorescence-activated cell sorting (FACS) after one-week cell culture using a cell sorter (Sony, SH800S Cell Sorter, San Jose, CA, USA). Quantification of cell cycle phases in MCF-7 and HCC1143 FUCCI reporter cells lines was performed by CellProfiler.

Bioinformatics analysis of Gene functional enrichment and annotation

Enrichment analysis was performed on the Metascape platform (https://metascape.org/gp/index.html#/main/step1) [20]. Pathway analysis was performed by Ingenuity Pathway Analysis software (IPA; QIAGEN), and in R with the clusterProfiler package using the Kyoto Encyclopedia of Genes and Genomes (KEGG) database. Protein-protein interaction (PPI) networks were analyzed using STRING database (https://string-db.org/). The *cytoHubba* plugin in Cytoscape software (version 3.7.2) was used to identify hub genes and their networks. The "Degree" algorithm was used to select the top genes in Cytoscape.

Analysis of clinical associations of hub genes

The association of the mean expression of the hub genes in each category selected from Cytoscape (gene networks derived from DEGs in acute or chronic hypoxia in MCF-7 or HCC1143 cells) in breast cancer patients with relapse-free survival (RFS) was analyzed using the Kaplan-Meier (KM) plotter platform (https://kmplot.com/analysis/). Logrank <0.01 was considered significant for difference between high and low expressors.

Statistical analysis

All statistical analysis was performed using GraphPad Prism 9 using t-test or one-way ANOVA. All experiments were performed at least three biological replicates where not indicated. Data were expressed as mean ± SD. Significance was indicated by **** ($p<0.0001$), *** ($p<0.001$), ** ($p<0.01$), * ($p<0.05$), and ns (not significant).

Results

Luminal and basal A breast cancer cells respond to acute and chronic hypoxia

To characterize the effects of acute and chronic hypoxia in breast cancer cells, we selected two representative human breast cancer cell lines for the luminal (MCF-7) and basal A (HCC1143) subtypes [21]. The cells were exposed to normoxia (21% O_2) or hypoxia (1% O_2) for acute (24 hrs) and chronic (5 days) periods. RNA was collected for transcriptomics analysis using TempO-Seq high throughput targeted sequencing technology [17]. Using the DESeq2 R package, DEGs in hypoxia when compared to normoxia were identified. To ensure that cells had experienced hypoxic conditions, we analyzed the expression of key hypoxic biomarkers including HIF1α and its target gene, CA9. CA9 mRNA expression was significantly increased in the TempO-Seq data in response to acute hypoxia and further increased in response to chronic hypoxia for both subtypes (Fig. 1A). This pattern was validated at the protein level by Western blot (Fig.1B). In agreement, HIF1α immunostaining showed increased accumulation in the

nuclei of both cell lines exposed to acute hypoxia and this early, rapid response was not further increased by chronic exposure (Fig.1C).

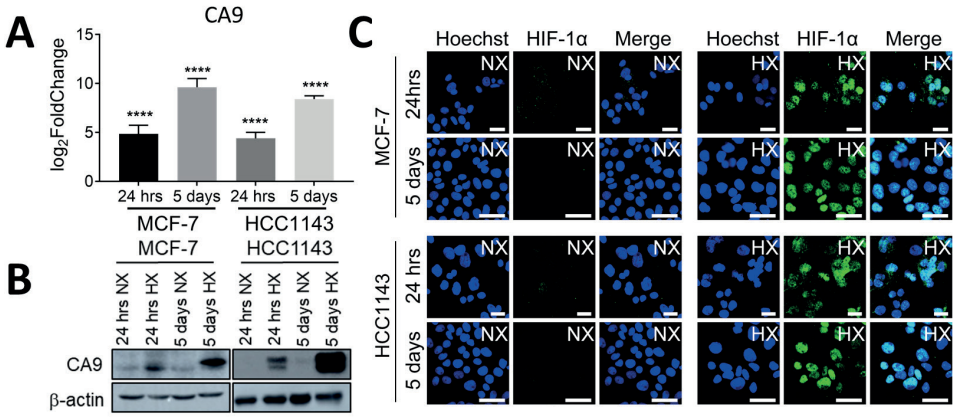

Figure 1. CA9 expression and activation of HIF1α signaling under acute and chronic hypoxia in MCF-7 and HCC1143 cell lines. (A) CA9 RNA expression in 4 datasets of transcriptome data, including MCF-7 24 hrs (MCF-7 24 hrs hypoxia normalized to MCF-7 24 hrs normoxia), HCC1143 24 hrs (HCC1143 24 hrs hypoxia normalized to HCC1143 24 hrs normoxia), MCF-7 5 days (MCF-7 5 days hypoxia normalized to MCF-7 5 days normoxia), HCC1143 5 days (HCC1143 5 days hypoxia normalized to HCC1143 5 days normoxia). Three biological replicates for each dataset; ****, padj <0.0001. **(B, C)** CA9 protein expression detected by western blotting (B) and Immunofluorescence of HIF1α localization by confocal microscopy (C) after 24 hrs (acute) and 5 days (chronic) incubation under normoxia (NX) and hypoxia (HX) in MCF-7 and HCC1143 cell lines. Blue, Hoechst; Green, HIF1α Ab. One representative experiment of three biological replicates is shown.

Differential activation of gene expression patterns in response to acute versus chronic hypoxia

Having validated that both cell lines were sensitive to the hypoxic environment, the impact of the duration of exposure was addressed. In both subtypes, chronic hypoxia led to a higher number of DEGs (|$\log_2$Foldchange| >1; padj < 0.05) as compared to acute hypoxia (MCF-7, 1880 vs 135 DEGs (Fig. 2A); HCC1143, 4947 vs 23 DEGs). Given the high number of DEGs in the HCC1143 5-days dataset, for subsequent further analysis using bioinformatics tools, for this dataset 2380 DEGs identified with more stringent |$\log_2$Foldchange| > 2 and padj <0.01 criteria were used (Fig. 2A). Interestingly, the switch from acute to chronic hypoxia led to a switch from a limited number of predominantly upregulated genes to a large number of predominantly downregulated genes in HCC1143 cells. Only 6 genes (NDRG1, CA9, IGFBP3, LOX, EGLN3, PPFIA4) overlapped between the 4 datasets and GO term analysis showed that these were all enriched in the HIF1 pathway (Fig. 2C, D). NDRG1, CA9, IGFBP3, LOX and EGLN3 were up-regulated in all 4 datasets, whereas PPFIA4 was up-regulated in MCF-7 but down-regulated in HCC1143 cells (Fig. 2C). For HCC1143 cells, 16 genes overlapped between acute and chronic hypoxia, and most of these were upregulated (Fig. 2E, F). These 16 genes were not only enriched in the HIF1α pathway but also in the Growth hormone synthesis, secretion, and action pathway (Fig. 2F, G). For MCF-7 cells, 95 genes overlapped between 24hrs and 5 days of hypoxic injury (Fig. 2H), of which 50 genes

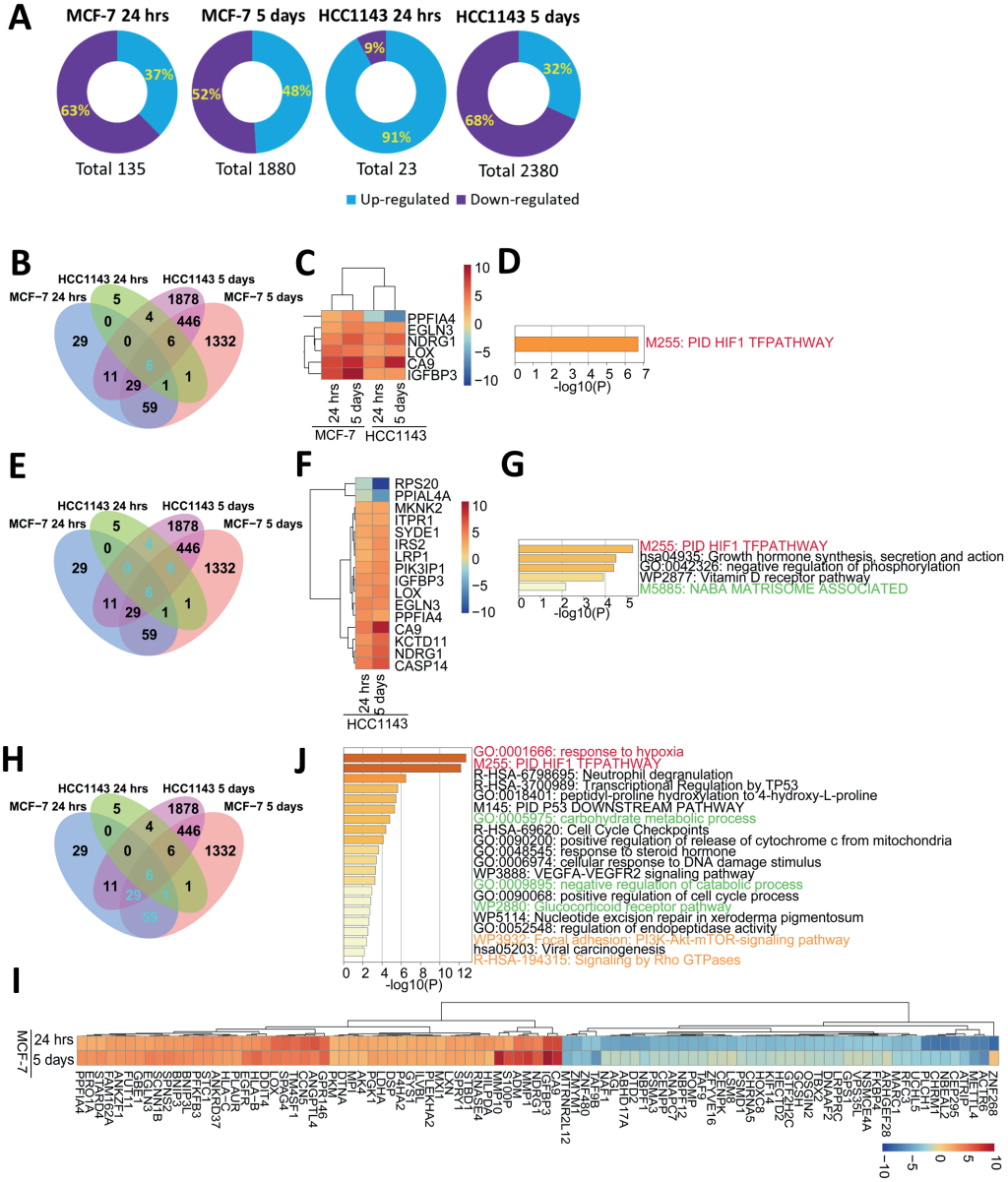

Figure 2. Transcriptome analysis of acute and chronic hypoxia in MCF-7 and HCC1143 cells. (A) Pie charts of up- and down-regulated DEGs in 4 datasets, including MCF-7 24 hrs, HCC1143 24 hrs, MCF-7 5 days and HCC1143 5 days. **(B-D)** Venn diagram of 4 datasets showing 6 shared DEGs in cyan (B) with associated heatmap (C), and top clusters of enriched terms (D). **(E-G)** Venn diagram of 4 datasets showing 4+6+6 shared DEGs for HCC1143 cells 24 hrs and 5 days hypoxia in cyan (E) with associated heatmap (F), and top clusters of enriched terms (G). **(H-J)** Venn diagram of 4 datasets showing 1+6+29+59 shared DEGs for MCF-7 cells 24 hrs and 5 days hypoxia in cyan (H) with associated heatmap (I), and top clusters (J). Enrichment analysis (D, G, J) was done by Metascape. Enriched items associated with HIF signaling, metabolism, and cytoskeleton are labelled in red, green and orange, respectively.

were upregulated and 44 genes were downregulated (Fig. 2I). These 95 genes were enriched in response to hypoxia, HIF1α pathway, carbohydrate metabolic process and cell cycle checkpoints (Fig. 2J). These data indicated that acute hypoxic stress triggered early adaptation by activation of the HIF1α pathway and chronic hypoxia led to further adaptation e.g., including proliferation and metabolism.

Differential response to hypoxia for basal A and luminal cells

We analyzed the DEGs using IPA to map the responses to hypoxia. Activation of HIF-1α signaling was a common response in both cell lines exposed to acute hypoxia and cell cycle regulation was affected by chronic hypoxia in both cell lines (Fig. 3A, C and E). Several other pathways were differentially affected in these cell lines. Interestingly, in MCF-7 cells exposed to chronic hypoxia changes in metabolic processes including glycolysis and cholesterol biosynthesis were dominant (Fig 3A and B) whereas these did not appear in HCC1143 cells, where, instead pathways related to the cytoskeleton such as ILK Signaling appeared (Fig. 3A and D). Subsequently, KEGG pathway analysis was used. In agreement with the results obtained using IPA, metabolism was affected in MCF-7 (Fig. 3F) while regulation of the actin cytoskeleton was affected in HCC1143 cells after 5 days of hypoxia (Fig. 3G). These data indicated that MCF-7 and HCC1143 shared an acute activation of the HIF1α pathway and subsequent changes in cell cycle regulation but also showed distinct responses to chronic hypoxia with more metabolic reprogramming in MCF-7 and cytoskeletal adaptation in HCC1143 cells.

Identification of hypoxia related hub genes and their clinical relevance

Cytoscape (*cytoHubba*) was used to identify and select hub genes with the Degree method [22]. Because of the different numbers of DEGs depending on the duration of hypoxia, we selected the top 10 and top 20 genes for acute and chronic hypoxia, respectively, and displayed them in their corresponding network (Fig. 4A). In the acute phase, hub genes in both cell lines contained several targets of HIF1α signaling, including CA9, IGFBP3, LOX, PFKFB3, PKM, and SLC16A3. In response to chronic hypoxia, hub genes diverged between the two cell lines except for genes related to cell proliferation such as EGFR, cyclin B1 (CCNB1) and cyclin D1 (CCND1). In agreement with pathway analysis (Fig. 3), GAPDH, a key metabolic enzyme in the glycolysis pathway was among the top 10 hub genes in MCF-7 and ACTB, encoding β-actin, was a prominent hub gene in HCC1143. Next, clinical relevance of the identified hub genes was analyzed using the Kaplan-Meier plotter platform. The mean expression of the 4 classes of hub genes (associated with acute or chronic hypoxia in MCF-7 or HCC1143) was significantly, negatively associated with relapse-free survival (RFS), with HR >1.2 and log Rank p <0.01 (Fig. 4B). These findings validated the prognostic value of the newly identified hypoxia related hub genes in breast cancer patients.

Chronic hypoxia impairs breast cancer cell proliferation

Our transcriptomics analysis revealed that altered expression of cell cycle related genes was a common response to acute and chronic hypoxia for both cell lines. We established FUCCI reporter MCF-7 and HCC1143 cell lines to address the impact of hypoxia on the cell cycle. Using confocal microscopy, distribution across cell cycle phases was quantified at 1, 3 and 5 days under normoxia and hypoxia. HCC1143 contained a larger fraction of

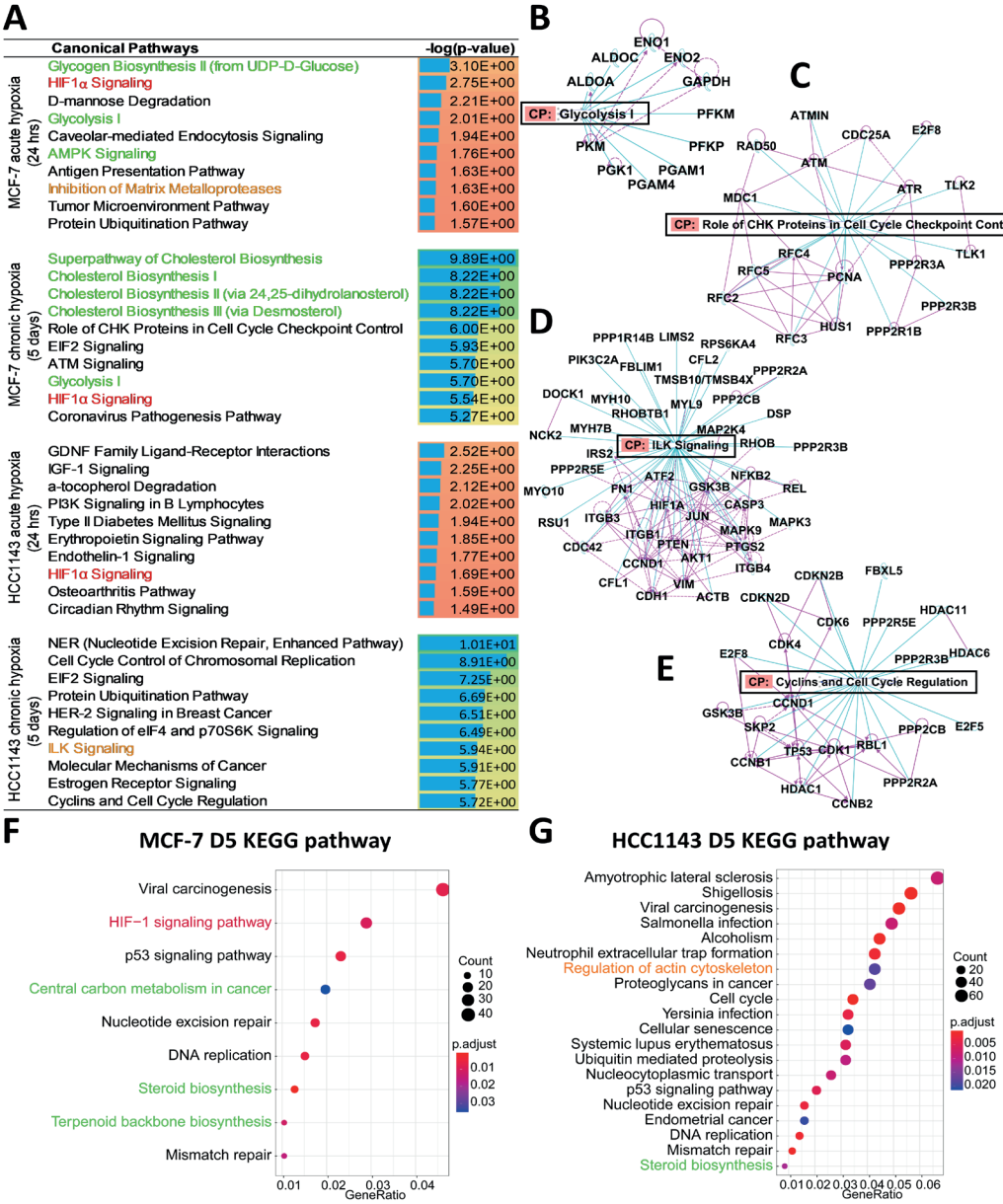

Figure 3. Pathway analysis of acute and chronic hypoxia in MCF-7 and HCC1143 cell lines. (A) Top10 Canonical pathways identified by IPA ranked by p-value in acute and chronic hypoxia in MCF-7 and HCC1143 cell lines. The color range from orange to yellow to green reflects –log(p-value) from low to high. The longer of the blue bar reflects the higher –log(p-value). **(B-E)** Networks with gene interactions indicated by pink lines drawn by IPA for canonical pathways, including Glycolysis (B) and Role of CHK protein in cell cycle checkpoint control (C) in MCF-7 cells exposed to chronic hypoxia; and ILK signaling (D) and Cyclins and cell cycle regulation (E) in HCC1143 cells exposed to chronic hypoxia. **(F, G)** KEGG pathway analysis in chronic hypoxia in MCF-7 (F) and HCC1143 (G) cells. Pathways associated with HIF signaling (red), metabolism (green), and cytoskeleton (orange) are marked both in IPA (A) and KEGG (F, G).

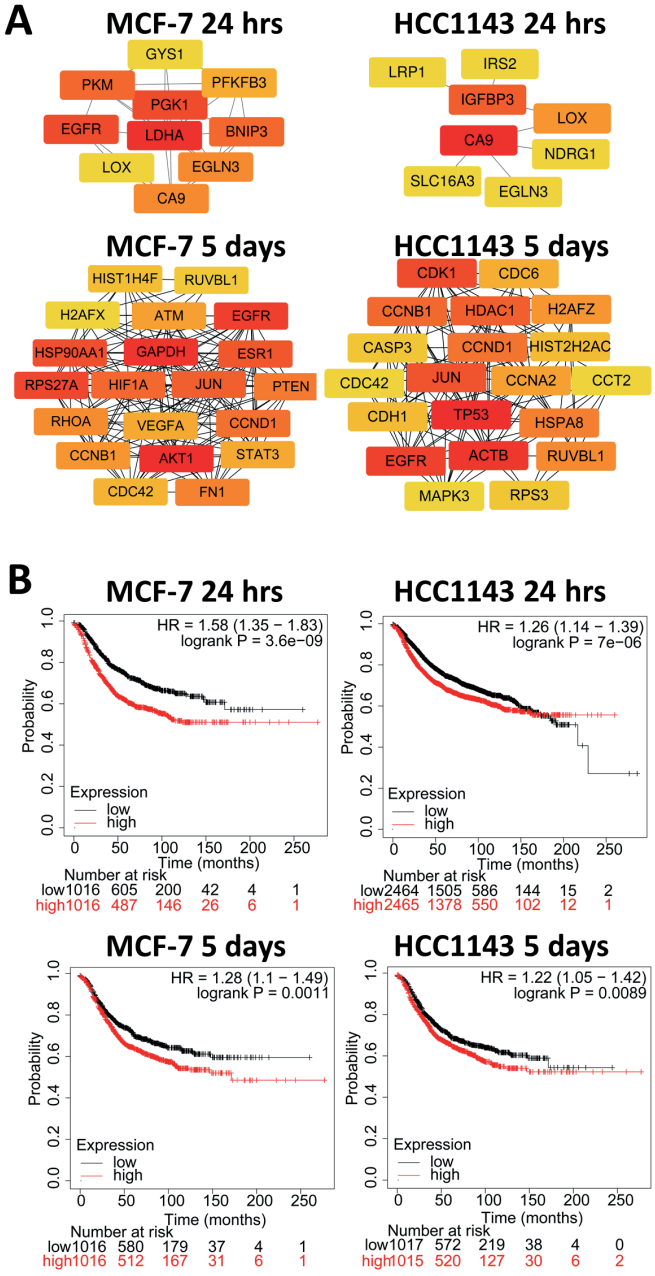

Figure 4. Hub genes of acute and chronic hypoxia in MCF-7 and HCC1143 cell lines. (A) Hub genes were calculated by Degree algorithm using Cytoscape (*cytoHubba*) software, top10 and top20 genes were picked for 24hrs (acute) and 5 days (chronic) hypoxia, respectively in MCF-7 and HCC1143 cell lines. The color of the genes from red to yellow is the rank of the genes from top to low. **(B)** Relapse-free survival (RFS) curves for hub genes drawn on the Kaplan-Meier (KM) plotter platform, for breast cancer patients. Mean expression of hub genes was used. Logrank <0.01 was considered significant for difference between high and low expressors.

cells in S-G2-M than MCF-7 and this fraction decreased progressively under normoxia as confluency was reached (Fig. 5A-D). In both cell lines, 3- and 5-days culture in hypoxia led to a stronger reduction in the fraction of cells in S-G2-M. In MCF-7 the fraction of cells in G1-S was also reduced under hypoxia but this was not observed in HCC1143. The apparent reduction in S phase was accompanied by a concomitant increase in unlabeled cells, pointing to an arrest in early G1 that was more prominent in hypoxia (Fig. 5).

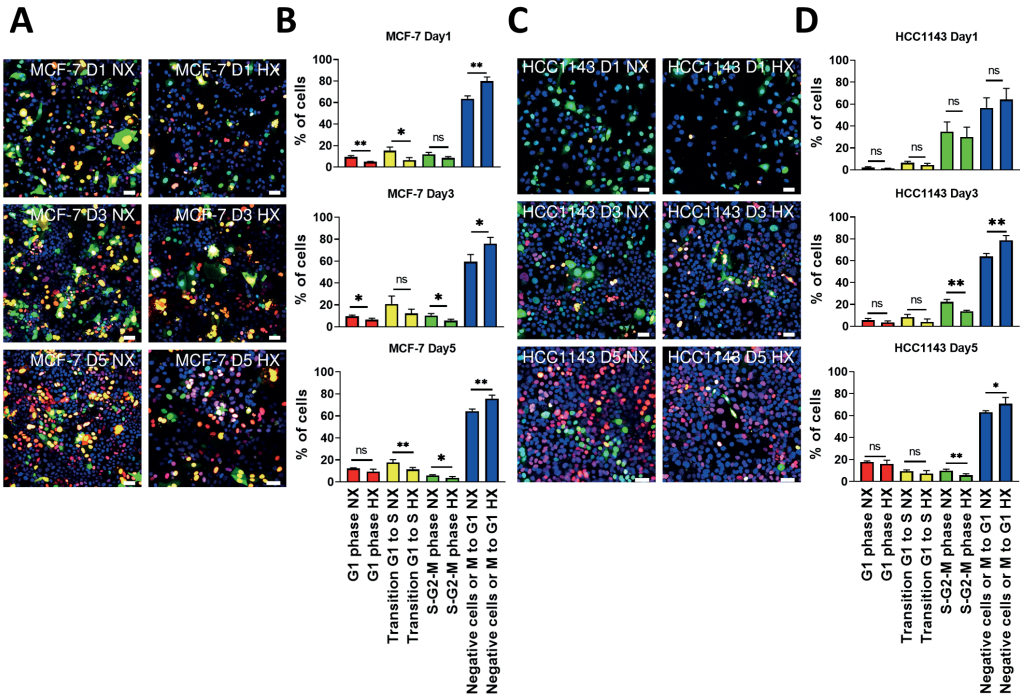

Figure 5. Cell phases in acute and chronic normoxia and hypoxia in MCF-7 and HCC1143 cell lines. (A, C) MCF-7 FUCCI reporter (A) and HCC1143 FUCCI reporter cells (C) were grown in normoxia (NX) and hypoxia (HX) for 1 day, 3 days and 5 days. Microscopy images show cell cycle phases marked by red (arrested in G1), yellow (transition G1 to S), green (S-G2-M), and blue nuclei (no staining; M-G1). **(B, D)** Quantification of cell cycle phases in MCF-7 (B) and HCC1143 (D) by Cellprofiler. Error bars indicate SD for triplicate measurements. **, p <0.01; *, p <0.05; ns, not significant.

Metabolic adaptation of luminal breast cancer cells under chronic hypoxia

Based on the transcriptomics data, chronic hypoxia differentially affected MCF-7 and HCC1143 cells with a predicted effect on glycolysis particularly in MCF-7 (Fig. 3 and 4). Indeed, several genes related to glycolysis were upregulated in response to chronic hypoxia, uniquely in MCF-7 (Fig. 6A). Conversely, in agreement with the predicted alteration on cytoskeleton organization, several genes associate with cytoskeletal organization, adhesion, and migration were upregulated in response to chronic hypoxia, uniquely in HCC1143 (Fig. 6B). To address whether this distinction reflected differences between breast cancer subtypes in the response to hypoxia, we first measured lactate levels in three luminal (MCF-7, T47D and BT474) and three basal A cell lines (HCC1143, SUM149PT and HCC1806). Average lactate production for all luminal cells under normoxia was lower when compared to the basal A breast cancer cells suggesting that

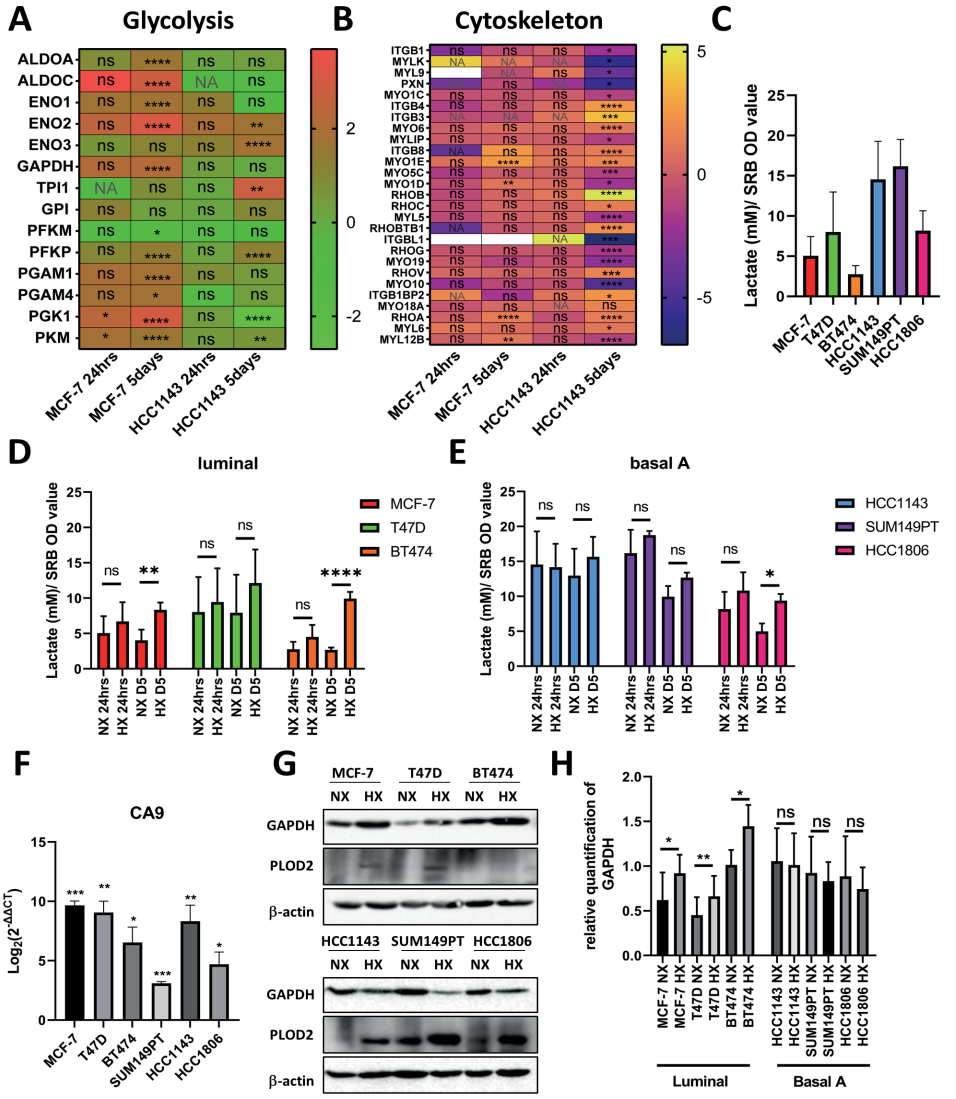

Figure 6. Chronic hypoxia affects metabolism in luminal breast cancer cells. (A, B) Heatmap of genes involved in glycolysis (A) and cytoskeleton (B) pathways in 24hrs (acute) and 5 days (chronic) hypoxia in MCF-7 and HCC1143 cells. NA, not available; ****, padj <0.0001; ***, padj <0.001; **, padj <0.01; *, padj <0.05; ns, not significant. White color means that genes were filtered out in targeted RNA sequencing data after filtering by DESeq2 package in R software. **(C)** Lactate levels (mM) in 6 cell lines under normoxia normalized to the OD value determined in SRB assay. **(D, E)** Lactate levels measured in 3 luminal (MCF-7, T47D, BT474) (D) and 3 basal A (HCC1143, SUM149PT, HCC1806) (E) breast cancer cell lines under acute normoxia/hypoxia and chronic normoxia/hypoxia normalized to the OD value determined in SRB assay. **(F)** CA9 RNA expression level under hypoxia in luminal and basal A cell lines detected by qRT-PCR. $Log_2(2^{-\Delta\Delta CT})$ was calculated by normalizing to normoxia in each cell line. Error bars indicate SD for triplicate measurements. ***, p <0.001; **, p <0.01; *, p <0.05. **(G)** GAPDH and PLOD2 protein expression detected by Western blot. β-actin serves as loading control. **(H)** Quantification of GADPH signal normalized to β-actin with Image J. Error bars indicate SD for triplicate measurements. **, p <0.01; *, p <0.05; ns, not significant.

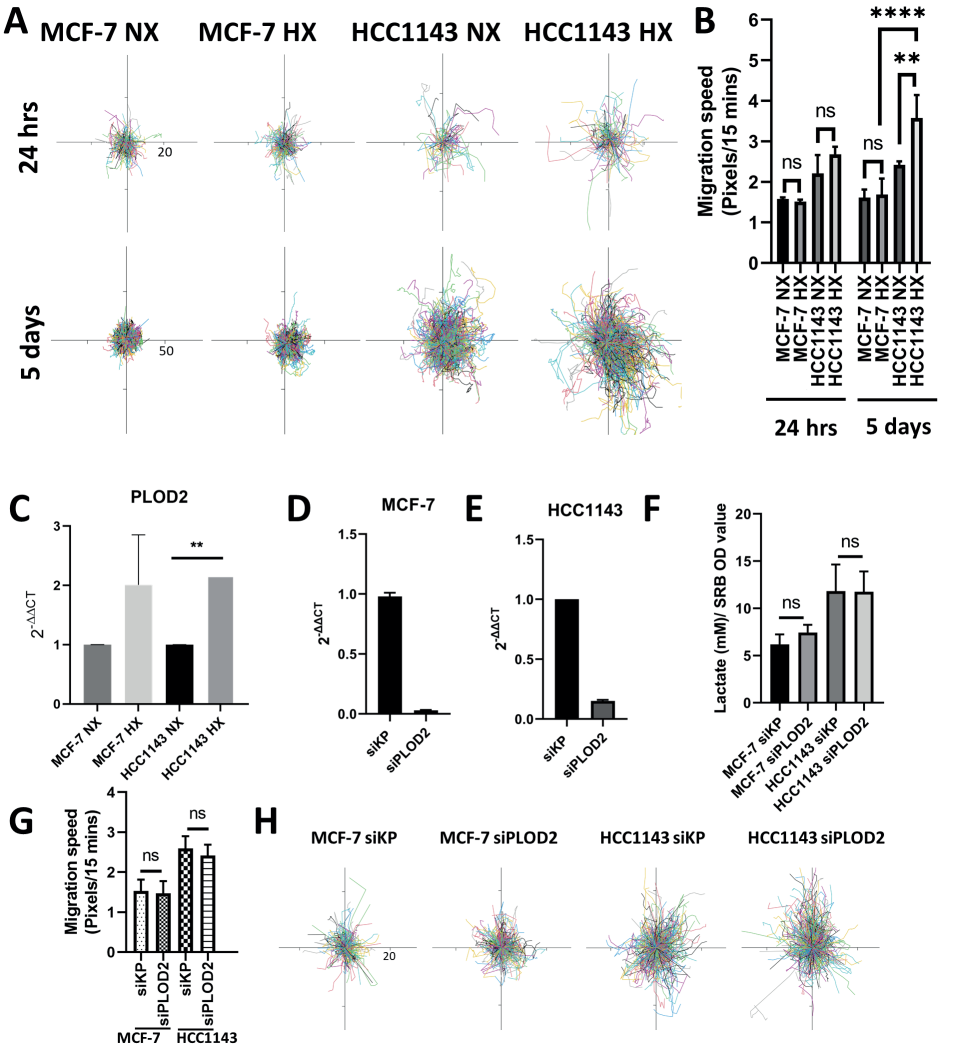

Figure 7. Chronic hypoxia affects cell migration in basal breast cancer cells. (A, B) Cell tracking of MCF-7 and HCC1143 cell lines in acute (24 hrs) and chronic hypoxia (5 days) (A), and calculated migration speed (B). Error bars indicate SD for triplicate measurements. ****, p <0.0001; **, p <0.01; ns, not significant. The pixels of acute hypoxia are 20 and of chronic hypoxia are 50 for cell tracking. **(C)** PLOD2 mRNA expression level detected by qRT-PCR in MCF-7 (two biological replicates) and HCC1143 cells (three biological replicates) comparing chronic hypoxia to normoxia. Error bars indicate SD for triplicate measurements. **, p <0.01. **(D, E)** PLOD2 mRNA expression level in MCF-7 (D) and HCC1143 (E) cells under chronic hypoxia in presence of PLOD2 siRNA or control "kinasepool" siRNA (siKP). Average and SD from two biological replicates are shown. **(F)** Lactate levels measured for the indicated cell lines under chronic hypoxia normalized to the OD value determined in SRB assay. **(G, H)** Migration speed (G) and cell tracking (20 pixels) (H) analyzed for the indicated cell lines under chronic hypoxia. ns, not significant. Error bars indicate SD for triplicate measurements. ns, not significant.

luminal cells were less glycolytic (Fig. 6C). Acute hypoxia did not influence lactate production in any of the breast cancer cell lines (Fig. 6D and E). The luminal breast cancer cell lines produced more lactate under chronic hypoxia (although this trend was not significant in T47D), whereas among the basal cell lines, HCC1806 (which had relatively low levels under normoxia) showed a significant increase under hypoxia and the two other basal cell lines (displaying high levels under normoxia) showed no change in lactate levels in response to hypoxia. To further address the apparent trend towards a selective increase in glycolysis in luminal cells, expression of GAPDH, a HIF1α regulated enzyme involved in glycolysis was analyzed. While hypoxia increased CA9 mRNA in all 6 cell lines as expected (Fig. 6F) GAPDH protein levels increased significantly in all three luminal cell lines but were unaffected in the basal A cell lines panel (Fig. 6G and H). These data point to increased glycolysis in response to chronic hypoxia particularly in luminal breast cancer cells.

Increased motility of HCC1143 cells under chronic hypoxia

To address the predicted changes in cytoskeletal organization (Fig. 3, 4 and 6B) in HCC1143 cells, the actin filament organization was analyzed in 3 luminal and 3 basal A cell lines cultured 5 days both under normoxia or hypoxia. In the three basal A cell lines (Fig. S1B) chronic hypoxia led to a more elongated morphology and an increase in stress fiber formation whereas the actin cytoskeleton remained unchanged in the three luminal lines (Fig. S1A). We next asked whether the change in cytoskeletal morphology affected the migratory behavior of the basal A cells. Indeed, cell migration speed, which was already higher in HCC1143 as compared to MCF-7 cells, was increased in response to chronic hypoxia exclusively in the basal A cells (Fig.7A and B). PLOD2 is a membrane-bound hydroxylase involved in extracellular matrix crosslinking that has been implicated in cancer cell migration [23] as well as glycolysis [24]. Transcriptomics analysis identified PLOD2 as a DEG induced by chronic hypoxia in MCF-7 whereas it was not significantly changed in HCC1143 cells (not shown). Induction of PLOD2 mRNA in response to chronic hypoxia in MCF-7 was confirmed by qPCR and this showed a similar response in HCC1143 cells (Fig. 7C). Western blot analysis further validated upregulation of PLOD2 in response to chronic hypoxia in 3 luminal and, more drastically, in 3 basal A cell lines (Fig. 6G). As PLOD2 could connect metabolic adaptation to changes in migration we investigated its role in the response to hypoxia in the luminal and basal A cells. However, siRNA-mediated silencing of PLOD2 in MCF-7 and HCC1143 cells did not affect lactate production or migration speed under chronic hypoxia (Fig.7D-H) arguing against such a role. Altogether, these data show that a shared response to hypoxia affecting the HIF1α pathway and cell cycle progression in breast cancer cells, is accompanied by distinct responses to chronic hypoxia with enhanced glycolysis predominantly in luminal cells and a promigratory switch predominantly in basal breast cancer cells.

Discussion

Hypoxia, a common feature in breast cancer can be divided into acute, chronic and intermittent hypoxia [9,25]. Thus far, research has largely focused acute hypoxia when studying the effect of oxygen deprivation in breast cancer cells [26–29]. Yet, cells may adapt differently to the dynamic hypoxic environment, by changing either their metabolism [30], decreasing cell proliferation [31] or becoming more invasive [5]. There is a limited number of studies investigating the differential response of breast cancer

cells to acute and chronic hypoxia [32,33].

In this study, we performed high throughput targeted RNA sequencing (TempO-Seq) of luminal (MCF-7) and basal A (HCC1143) breast cancer cells cultured either 24 hrs or 5 days under hypoxic conditions. The influence of hypoxia on the cell cycle was verified using MCF-7 and HCC1143 FUCCI reporter cell lines. Both cell lines showed a reduced fraction in S-G2-M phase in chronic hypoxia and HCC1143 cells were arrested in the G1 phase. The cell cycle is a vital process that is influenced by cell shape [34], cytoskeletal tension [35], and metabolism [36], which are different between the two cell lines. Nevertheless, the impact of hypoxia on cell cycle phase distribution was similar for both cell lines.

Cancer cells produce energy by glycolysis instead of oxidative phosphorylation and our findings are in agreement with earlier studies showing that glycolysis is more prominent in basal A cells than in luminal cells [37,38]. We find that chronic hypoxia induces glycolysis in luminal cells but has little effect in (already more glycolytic) basal A cells in this respect. Indeed, GAPDH, a metabolic marker for glycolysis [39,40] is increased in response to chronic hypoxia in luminal but not basal A cells.

In basal A cells chronic hypoxia stimulates pathways associated with actin cytoskeletal organization and migration. The actin cytoskeleton generates pushing or pulling forces by actin polymerization or mutual sliding of actin and myosin II filaments to realize cell migration and morphogenesis [48–50]. Hypoxia has been shown to induce actin rearrangement and assembly of actin stress fiber via Rho GTPase signaling [51–54]. Our findings indicate that both several pathways involved in this process are affected by chronic hypoxia mainly in basal A cells. Indeed, cytoskeletal organization as well as cell migration are largely unaffected by hypoxia in luminal cells whereas they are strongly affected in basal A cells.

Our findings indicate that luminal cells respond mainly by changes in metabolism whereas basal A cells show pro-migratory changes. Interestingly, PLOD2, a glycolytic risk gene promoting glycolysis [24,41], that is induced by hypoxia and stimulates EMT in cancer [23,42] is triggered by hypoxia in luminal cells and more abundantly in basal A cells in our study. PLOD2 is involved in both metabolism and cytoskeletal organization and contributes to both glycolysis and cell migration under hypoxia [43–46]. Despite its upregulation we do not identify a functional role of PLOD2 in hypoxia-stimulated glycolysis or cell migration. Given its role in collagen cross linking its pro-migratory effect may be observed especially in 3D culture conditions.

In conclusion, we explored different subtypes breast cancer cell lines under acute and chronic hypoxia. Chronic hypoxia mainly affects cytoskeleton in basal A cells and metabolism in luminal cells, which is further confirmed by higher cell migration speed and more F-actin stress fibers in basal A cells and by more lactate productivity and increased GADPH in luminal cells. Our study provides a new insight in understanding the biology of breast tumors in a hypoxic environment.

Acknowledgments
The authors thank Hans de Bont from LACDR at Leiden University for technical assistance with microscopy; Sylvestre Bonnet from LIC at Leiden University for sharing the hypoxia incubator. Qiuyu Liu and Nasi Liu were financially supported by the China Scholarship Council.

Competing Interests
On behalf of all authors, the corresponding author states that there is no conflict of interest.

Author contributions
Qiuyu Liu: writing original draft, conducting experiments, analysing data; Nasi Liu: quantifying cell migration assay; Vera van der Noord: establishing analysis pipeline of cell cycle of FUCCI reporter cell lines; Wanda van der Stel: introducing lactate assay method; Bob van de Water: review manuscript; Erik HJ Danen & Sylvia E. Le Dévédec: writing original draft, review, supervision

Data Availability Statement
TempO-Seq data supporting the results of this article will be available in the BioStudies database from EMBL-EBI.

References
1.Azamjah, N., Soltan-Zadeh, Y. & Zayeri, F. Global Trend of Breast Cancer Mortality Rate: A 25-Year Study. Asian Pacific journal of cancer prevention: APJCP 20, 2015–2020 (2019).
2.Hanahan, D. Hallmarks of Cancer: New Dimensions. Cancer discovery 12, 31–46 (2022).
3.Mosier, J. A., Schwager, S. C., Boyajian, D. A. & Reinhart-King, C. A. Cancer cell metabolic plasticity in migration and metastasis. Clinical & experimental metastasis 38, 343–359 (2021).
4.Al Tameemi, W., Dale, T. P., Al-Jumaily, R. M. K. & Forsyth, N. R. Hypoxia-Modified Cancer Cell Metabolism. Frontiers in cell and developmental biology 7, 4 (2019).
5.Nagelkerke, A. et al. Hypoxia stimulates migration of breast cancer cells via the PERK/ATF4/LAMP3-arm of the unfolded protein response. Breast cancer research : BCR 15, R2 (2013).
6.Tam, S. Y., Wu, V. W. C. & Law, H. K. W. Hypoxia-Induced Epithelial-Mesenchymal Transition in Cancers: HIF-1α and Beyond. Frontiers in oncology 10, 486 (2020).
7.Lin, Q., Cong, X. & Yun, Z. Differential hypoxic regulation of hypoxia-inducible factors 1alpha and 2alpha. Molecular cancer research : MCR 9, 757–765 (2011).
8.Muz, B., La Puente, P. de, Azab, F. & Azab, A. K. The role of hypoxia in cancer progression, angiogenesis, metastasis, and resistance to therapy. Hypoxia (Auckland, N.Z.) 3, 83–92 (2015).
9.Saxena, K. & Jolly, M. K. Acute vs. Chronic vs. Cyclic Hypoxia: Their Differential Dynamics, Molecular Mechanisms, and Effects on Tumor Progression. Biomolecules 9 (2019).
10.Bayer, C. & Vaupel, P. Acute versus chronic hypoxia in tumors: Controversial data concerning time frames and biological consequences. Strahlentherapie und Onkologie : Organ der Deutschen Rontgengesellschaft ... [et al] 188, 616–627 (2012).
11.Ji, W. et al. Effects of acute hypoxia exposure with different durations on activation of Nrf2-ARE pathway in mouse skeletal muscle. PloS one 13, e0208474 (2018).
12.Reiterer, M. et al. Acute and chronic hypoxia differentially predispose lungs for metastases. Scientific reports 9, 10246 (2019).
13.Taube, J. H. et al. Core epithelial-to-mesenchymal transition interactome gene-expression signature is associated with claudin-low and metaplastic breast cancer subtypes. Proceedings of the National Academy of Sciences of the United States of America 107, 15449–15454 (2010).
14.Wu, Y., Sarkissyan, M. & Vadgama, J. V. Epithelial-Mesenchymal Transition and Breast Cancer. Journal of clinical medicine 5 (2016).
15.Takatani-Nakase, T. et al. Hypoxia enhances motility and EMT through the Na+/H+ exchanger NHE-1 in MDA-MB-231 breast cancer cells. Experimental cell research 412, 113006 (2022).
16.Kierans, S. J. & Taylor, C. T. Regulation of glycolysis by the hypoxia-inducible factor (HIF): implications for cellular physiology. The Journal of physiology 599, 23–37 (2021).
17.Yeakley, J. M. et al. A trichostatin A expression signature identified by TempO-Seq targeted whole transcriptome profiling. PloS one 12, e0178302 (2017).
18.Carpenter, A. E. et al. CellProfiler: image analysis software for identifying and quantifying cell phenotypes. Genome biology 7, R100 (2006).
19.Wink, S. et al. Quantitative high content imaging of cellular adaptive stress response pathways in toxicity for chemical safety assessment. Chemical research in toxicology 27, 338–355 (2014).
20.Zhou, Y. et al. Metascape provides a biologist-oriented resource for the analysis of systems-level datasets. Nature communications 10, 1523 (2019).
21.Dai, X., Cheng, H., Bai, Z. & Li, J. Breast Cancer Cell Line Classification and Its Relevance with Breast Tumor Subtyping. Journal of Cancer 8, 3131–3141 (2017).
22.Xi, Y., Liu, J. & Shen, G. Low expression of IGFBP4 and TAGLN accelerate the poor overall survival of osteosarcoma. Scientific reports 12, 9298 (2022).
23.Gilkes, D. M. et al. Procollagen lysyl hydroxylase 2 is essential for hypoxia-induced breast cancer metastasis. Molecular cancer research : MCR 11, 456–466 (2013).
24.Du, W. et al. PLOD2 promotes aerobic glycolysis and cell progression in colorectal cancer by upregulating HK2.

Biochemistry and cell biology = Biochimie et biologie cellulaire 98, 386–395 (2020).
25.Peir, C. H. F. et al. The role of hypoxia-induced factor 1 in breast cancer. JCMT 2019 (2019).
26.Karlenius, T. C., Shah, F., Di Trapani, G., Clarke, F. M. & Tonissen, K. F. Cycling hypoxia up-regulates thioredoxin levels in human MDA-MB-231 breast cancer cells. Biochemical and biophysical research communications 419, 350–355 (2012).
27.Han, J. et al. Hypoxia is a Key Driver of Alternative Splicing in Human Breast Cancer Cells. Scientific reports 7, 4108 (2017).
28.Cooper, C. et al. Intermittent hypoxia induces proteasome-dependent down-regulation of estrogen receptor alpha in human breast carcinoma. Clinical cancer research : an official journal of the American Association for Cancer Research 10, 8720–8727 (2004).
29.Azimi, I., Petersen, R. M., Thompson, E. W., Roberts-Thomson, S. J. & Monteith, G. R. Hypoxia-induced reactive oxygen species mediate N-cadherin and SERPINE1 expression, EGFR signalling and motility in MDA-MB-468 breast cancer cells. Scientific reports 7, 15140 (2017).
30.Takeda, K., Arase, S. & Takahashi, S. Side effects of topical corticosteroids and their prevention. Drugs 36 Suppl 5, 15–23 (1988).
31.Tang, K. et al. Hypoxia Promotes Breast Cancer Cell Growth by Activating a Glycogen Metabolic Program. Cancer research 81, 4949–4963 (2021).
32.Stiehl, D. P. et al. Non-canonical HIF-2α function drives autonomous breast cancer cell growth via an AREG-EGFR/ErbB4 autocrine loop. Oncogene 31, 2283–2297 (2012).
33.Jarman, E. J. et al. HER2 regulates HIF-2α and drives an increased hypoxic response in breast cancer. Breast cancer research : BCR 21, 10 (2019).
34.Clark, A. G. & Paluch, E. Mechanics and regulation of cell shape during the cell cycle. Results and problems in cell differentiation 53, 31–73 (2011).
35.Huang, S., Chen, C. S. & Ingber, D. E. Control of cyclin D1, p27(Kip1), and cell cycle progression in human capillary endothelial cells by cell shape and cytoskeletal tension. Molecular biology of the cell 9, 3179–3193 (1998).
36.Icard, P., Fournel, L., Wu, Z., Alifano, M. & Lincet, H. Interconnection between Metabolism and Cell Cycle in Cancer. Trends in biochemical sciences 44, 490–501 (2019).
37.Masson, N. & Ratcliffe, P. J. Hypoxia signaling pathways in cancer metabolism: the importance of co-selecting interconnected physiological pathways. Cancer & metabolism 2, 3 (2014).
38.Farhadi, P. et al. Cell line-directed breast cancer research based on glucose metabolism status. Biomedicine & pharmacotherapy = Biomedecine & pharmacotherapie 146, 112526 (2021).
39.Zhu, X., Jin, C., Pan, Q. & Hu, X. Determining the quantitative relationship between glycolysis and GAPDH in cancer cells exhibiting the Warburg effect. The Journal of biological chemistry 296, 100369 (2021).
40.Hjerpe, E. et al. Metabolic markers GAPDH, PKM2, ATP5B and BEC-index in advanced serous ovarian cancer. BMC clinical pathology 13, 30 (2013).
41.Xu, F. et al. The effect of a novel glycolysis-related gene signature on progression, prognosis and immune microenvironment of renal cell carcinoma. BMC cancer 20, 1207 (2020).
42.Du, H., Pang, M., Hou, X., Yuan, S. & Sun, L. PLOD2 in cancer research. Biomedicine & pharmacotherapy = Biomedecine & pharmacotherapie 90, 670–676 (2017).
43.Xu, F., Zhang, J., Hu, G., Liu, L. & Liang, W. Hypoxia and TGF-β1 induced PLOD2 expression improve the migration and invasion of cervical cancer cells by promoting epithelial-to-mesenchymal transition (EMT) and focal adhesion formation. Cancer cell international 17, 54 (2017).
44.Xu, Y. et al. Procollagen-lysine 2-oxoglutarate 5-dioxygenase 2 promotes hypoxia-induced glioma migration and invasion. Oncotarget 8, 23401–23413 (2017).
45.Wan, J. et al. Hypoxia-induced PLOD2 regulates invasion and epithelial-mesenchymal transition in endometrial carcinoma cells. Genes & genomics 42, 317–324 (2020).
46.Gilkes, D. M., Bajpai, S., Chaturvedi, P., Wirtz, D. & Semenza, G. L. Hypoxia-inducible factor 1 (HIF-1) promotes extracellular matrix remodeling under hypoxic conditions by inducing P4HA1, P4HA2, and PLOD2 expression in fibroblasts. The Journal of biological chemistry 288, 10819–10829 (2013).
47.Pollard, T. D. Actin and Actin-Binding Proteins. Cold Spring Harbor perspectives in biology 8 (2016).
48.Svitkina, T. M. Ultrastructure of the actin cytoskeleton. Current opinion in cell biology 54, 1–8 (2018).
49.Pellegrin, S. & Mellor, H. Actin stress fibres. Journal of cell science 120, 3491–3499 (2007).
50.Svitkina, T. The Actin Cytoskeleton and Actin-Based Motility. Cold Spring Harbor perspectives in biology 10 (2018).
51.Zieseniss, A. Hypoxia and the modulation of the actin cytoskeleton - emerging interrelations. Hypoxia (Auckland, N.Z.) 2, 11–21 (2014).
52.Hookham, M. B. et al. Hypoxia-induced responses by endothelial colony-forming cells are modulated by placental growth factor. Stem cell research & therapy 7, 173 (2016).
53.Glass, J. J., Phillips, P. A., Gunning, P. W. & Stehn, J. R. Hypoxia alters the recruitment of tropomyosins into the actin stress fibres of neuroblastoma cells. BMC cancer 15, 712 (2015).
54.Le Clainche, C. & Carlier, M.-F. Regulation of actin assembly associated with protrusion and adhesion in cell migration. Physiological reviews 88, 489–513 (2008).
55.Lehtimäki, J. I., Rajakylä, E. K., Tojkander, S. & Lappalainen, P. Generation of stress fibers through myosin-driven reorganization of the actin cortex. eLife 10 (2021).
56.Tojkander, S., Gateva, G. & Lappalainen, P. Actin stress fibers--assembly, dynamics and biological roles. Journal of cell science 125, 1855–1864 (2012).

Supplemental data

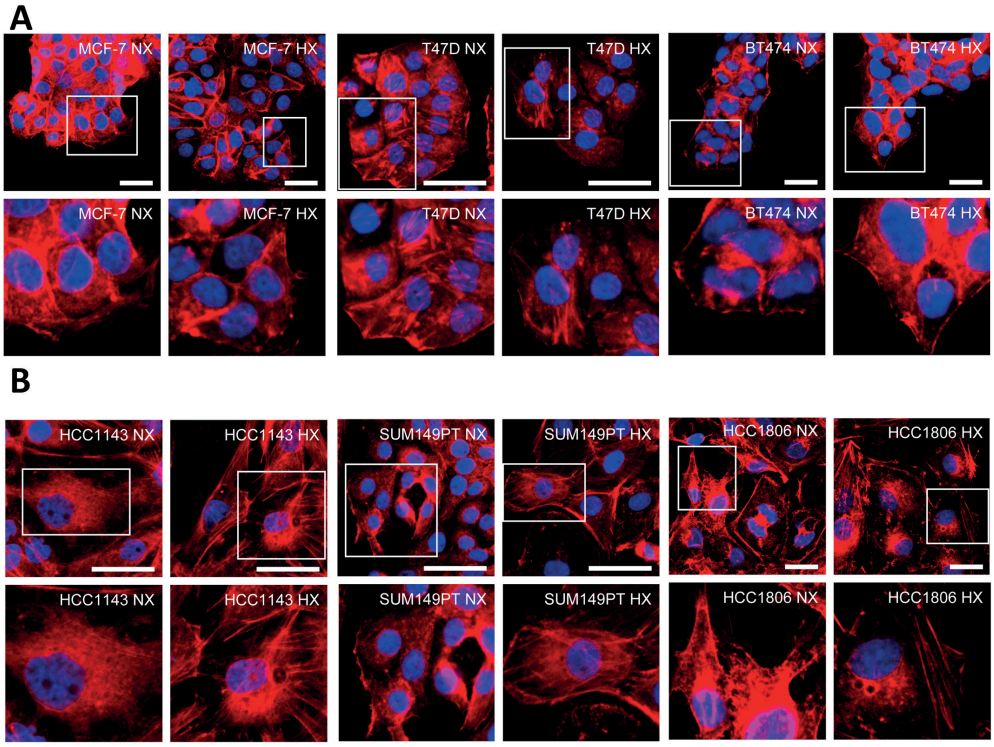

Figure S1. Chronic hypoxia affects actin cytoskeleton mainly in basal A breast cancer cells. (A, B) Phalloidin (red) and Hoechst (blue) staining of 3 luminal (MCF-7, T47D, BT474) (A) and 3 basal A (SUM149PT, HCC1806, HCC1143) (B) breast cancer cell lines grown under normoxia (NX) and hypoxia (HX) for 5 days.